PCCP

Accepted Manuscript

ROYAL SOCIETY OF CHEMISTRY

www.rsc.org/pccp

Electronic structures and current conductivities by B, C, N and F defects in amorphous titanium dioxide

Hieu H. Pham and Lin-Wang Wang
Joint Center for Artificial Photosynthesis and Materials Sciences Division
Lawrence Berkeley National Laboratory, Berkeley, California 94720

Corresponding Author: lwwang@lbl.gov (L.-W.W)

Abstract.
Although titanium dioxide (TiO_2) has been extensively studied and widely used in energy and environmental areas, the amorphous form and its related defect properties are poorly understood. Recent studies, however, have emphasized the crucial role of amorphousness in producing competitively good performance in photochemical applications. In this work we have investigated for the first time the effects of various dopants (B, C, N and F) on charge carrier transport in the amorphous titanium dioxide (a-TiO_2), given that doping is a common technique to tune the electronic properties of semiconductors and the existence of these impurities could also be unintentionally introduced during the synthesis process. The a-TiO_2 model was obtained using classical molecular dynamics method, followed by density-functional theory calculations (DFT+U, with Hubbard correction term U) on electronic structures and defect states. The doping's of these impurities were found to be more favorable in a-TiO_2 by several eV compared to their crystal counterparts (rutile). The contributions of these defect states to the charge transfer processes were examined by means of Marcus theory.

Keywords. transition metal oxides, polarons, defect states, electronic structure, Marcus theory, TiO_2, doping, charge transport

1. Introduction

Titanium dioxide (TiO_2) has shown broad applications for various technologies and engineering, including photosynthesis, solar cells, biomedical devices, rechargeable batteries, hydrogen storage and sensors [1, 2]. In comparison to the crystalline counterparts (rutile, brookite and anatase), the amorphous TiO_2 (a-TiO_2) has huge advantage for the large-scale production due to the cost-effectiveness of growth techniques as well as its ability to form smooth interface with substrates of different lattice constants. Although it was believed that the amorphicity could diminish the electrochemical activity, such as limiting the charge carrier lifetime and decreasing their mobilities; recent studies have shown otherwise, with reported improved a-TiO_2 efficiencies as photocatalysts, substrates and protection layers [3-10]. In particular, the role of amorphousness and defects states in the amorphous structure could be of great interests. For example, as reported lately [6], the ALD (atomic layer deposition) a-TiO_2 can be used as a protection layer of the photoanodes in solar cell water splitting while effectively conducting hole. In a previous study, our theoretical calculations have suggested that the oxygen vacancy might induce a mid-gap state via which the hole is conducted in this "leaky" a-TiO_2 thin film [11].

Due to the complexity to define the amorphous disorder and control its parameters, the electronic and photochemical properties of a-TiO_2 were not thoroughly characterized and it remains to be quite a challenging problem [12-22]. However, the fundamental understanding of its electronic structures and their correlations to the atomic structures is essential to improve the materials design and production, in particular to meet the high standards of next-generation devices for industrial-scale applications. In general, the effects of doping and defect introduction in crystals would be more straightforward that they could either significantly improve or degrade the materials' properties, including their energetics, chemical activities and mechanical performances [23, 24]. For TiO_2 crystals specifically, the issue of how to tune their photochemical properties with dopants has been extensively examined [25-37]. For instance, among well-established techniques is to dope TiO_2 with Nitrogen to narrow the band gap of rutile and anatase [26, 27, 33]. Nevertheless, the scenario might be very different and much more complicated when the amorphous phase is presented. Given that the contamination of lightweight impurities to some extent might be hard to avoid during the synthesis process, it is necessary to understand the effects of these defects in combination with the structural disorder. In this work, we have attempted to investigate specifically the behaviors of second-row elements (B, C, N and F) in the

amorphous TiO_2, their electronic states and possible contributions to the charge conduction process. Our *ab initio* calculations suggested that a-TiO_2 could be relatively easy to dope, with the dopant formation energies of several eV lower than those in their crystal (rutile) counterparts. Subsequently, the defect states induced by those impurities could be more prevalent in the amorphous phase. However, the calculations on charge transfer using the Marcus theory indicated that the electronic conductivities via these defect channels are quite low due to the localization nature of the charges.

2. Computational details

We used molecular dynamics (MD) simulation with classical force field to obtain the amorphous model of titanium dioxide. The interatomic potentials between Ti-Ti, Ti-O and O-O pairs are characterized by the Matsui-Akaogi force field [38], which has shown to successfully reproduce the structural properties of the crystals, as well as the liquid and amorphous TiO_2 [39]. The potential energy of this Matsui-Akaogi force field is described as a sum of pairwise contributions representing the Coulomb, dispersion and repulsion interactions. The amorphousness was produced using the "melt-and-quench" technique with the MD simulation, followed by further atomic relaxation by first-principles calculations. The detailed computational procedure on this "melt-and-quench" process, as well as the structural characterization of a-TiO_2, was presented and analyzed in our previous publication [11].

Density functional theory (DFT) [40] as implemented in the Vienna *ab initio* Simulation Package (VASP), [41] was employed to perform the first-principles calculations. The DFT calculations used the electron projector-augmented wave methods [42] with the PBE generalized gradient approximation (GGA) exchange–correlation functional [43], plus an on-site Ti d state U correction (DFT+U, or say GGA+U) [44]. The value of U = 4.2 was applied for the Coulomb correction to the Ti 3d states, which was reported to well describe the electronic properties and defect states in crystalline titanium dioxide [25, 45]. A plane-wave cut-off of 400 eV was used and the magnetic moment was accounted for by performing spin-polarized energy calculations. For the k-space sampling, we used a 2x2x3 Monkhorst-Pack grid [46] for both 216-atom rutile and amorphous TiO_2 supercells. For the calculations of charge mobility, we also performed the HSE06 calculation [47] which is expected to be more reliable than the GGA+U. Due to their relatively high computational cost, a single k-point (1x1x1) was used for the HSE06 calculations.

The formation energy of each impurity substitution (B, C, N and F in place of O) with charge state q is calculated as follows [48]:

$$\Delta H(I^q) = E(I^q) - E(clean) - (E_I + \mu_I) + (E_O + \mu_O) + q(\epsilon_{VBM} + E_F + \Delta v) \quad (1)$$

where $E(I^q)$ and $E(clean)$ are the total energies of the supercell with and without the impurity substitution. μ_I and μ_O are the elemental chemical potentials of the impurity (boron, carbon, nitrogen or fluorine) and oxygen, referenced to the elemental energy E_I and E_O of their ground states (we used the simple rhombohedral form of boron, graphite for carbon and gas phases for nitrogen, fluorine and oxygen). For simplicity, we assume B-, C-, N-, O-, F-rich conditions, i.e. μ = 0 for all cases. E_F is the Fermi energy level referenced to the valence band maximum (VBM) eigenenergy of the bulk TiO_2 system, and ϵ_{VBM} is the VBM eigen energy of the bulk system when the averaged Hartree potential is set to zero. The term Δv is added for the correction of the electrostatic interaction caused by the limited size of the supercell, obtained by taking the shifting of the 1s core-level energy of a Ti atom (located far away from the impurity site) between the neutral impurity and charged cases.

3. Results and Discussion

3.1. Defect states of impurity dopants in a-TiO_2

Figure 1 presents the calculations of formation energy for different impurity defects in the amorphous and rutile TiO_2, including B_{Ti} (replacement of Ti by B), C_{Ti} (replacement of Ti by C), C_O (replacement of O by C), N_O (replacement of O by N) and F_O (replacement of O by F). We have to mention that, in a-TiO_2, there are different sites to replace Ti and O, which tend to yield different formation energies. The reported formation energies in Figure 1 are the lowest ones for the corresponding impurity species. The substitution sites were chosen as described in the following procedure. It was found that the VBM and CBM of the amorphous TiO_2 are localized on some oxygen and titanium atoms instead of being delocalized all over the supercell [11]. Those O and Ti are used as the most favorable sites for impurity substitutions.

In Figure 1, only the charge state with lowest energy (at a specific Fermi energy) was plotted for each element. They all follow the trend that the formation of the impurity in a-TiO_2 is energetically more favorable (several eV lower) than its counterpart in the rutile phase. This suggests that the presence of these impurity atoms in the amorphous TiO_2 could be more prominent than its rutile counterpart.

The calculation shows that the B_{Ti} defect tends to be more stable at the -1 charge state in both phases, except when E_F is very close to the VBM in a-TiO_2 (Figure 1a). The substitution of Ti by B only induces the tail state at the VBM for the rutile crystal. On the contrary, the neutral B_{Ti} in a-TiO_2 results in a clear mid-gap state (Figure 2a), probably due to a more pronounced reconstruction of the local lattice. However, according to the formation energy calculations, this unoccupied orbital could be readily filled up as long as the Fermi energy is slightly above the VBM. Upon further lattice relaxation after this state is occupied, this state merges into the valence band and recovers a clean band gap. In other words, if the Ti^{4+} is first removed and then filled up by a B^{3+}, it will end up with a -1 charged state and this -1 charged state will not have any in-gap states as shown in Figure 3a. This observation is consistent with what was seen in other oxides or ionic materials [11, 49]: when the ion is removed by its ionic charged state, the system may not have an in-gap state after the structural relaxation. The C_{Ti}, meanwhile, can only have the neutral charge due to the identical number of valance electrons between C and Ti and no defect state is expected (Figure 2b, g). The substitution of Ti by C, therefore, might has little effect in terms of changing the electronic and transport properties of this system.

Unlike B_{Ti}, the transition between different charge states can be observed clearly in the middle of band gap for O replacement: C_O, N_O and F_O (Figure 1). The case of C_O deserves some attention here. When O is substituted by a neutral C in r-TiO_2, two orbitals are left empty and they would be seen as empty mid-gap states (Figure 2h). However, in the amorphous structure, those empty energy bands only exist before the structural optimization. After the lattice relaxation they are shifted up and merge into the CBM, and only occupied defect states could be seen (Figure 2c). The introduction of N_O (and F_O), nevertheless, results in an unoccupied (and occupied, respectively for F_O) defect state in both r-TiO_2 and a-TiO_2 due to the missing (or excess) of the electron (Figure 2 d, e, i, j).

Similar to B_{Ti}^{1-}, the formation of ionic F_O^{1+} induces no mid-gap state in both r-TiO_2 and a-TiO_2, after the structural and electronic relaxations were performed (Figure 3d, h). However, this is no more the case for C_O^{2-} and N_O^{1-}: the occupied defect states are observed in the middle of the band gap for both r-TiO_2 and a-TiO_2, even after the atomic structure is fully relaxed. Thus we see that, in addition to the isovalent case of C_{Ti}, there are no states inside the band gap for the more ionic cases of B_{Ti}^{1-} and F_O^{1+}. However, for the more covalent states of C_O^{2-} and N_O^{1-} the mid-gap states could still be seen.

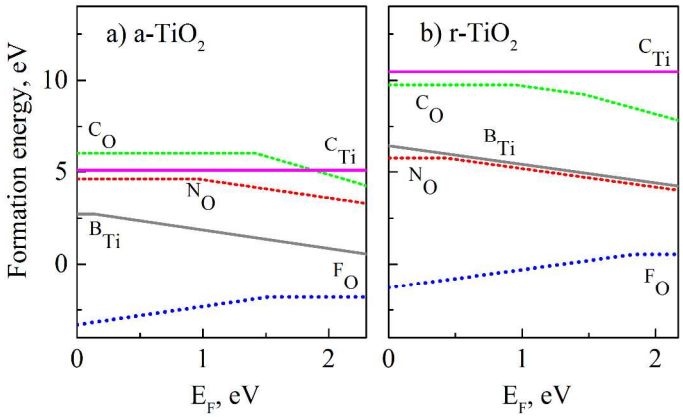

Figure 1. Formation energy of defects (B, C, N and F) as a function of Fermi energy in: a) amorphous TiO_2 and b) rutile TiO_2. The impurity-rich and O-rich conditions were used in equation (1). The turning points show the level of transition energy between different charge states. Positive slope means positively charged state, while negative slope means negatively charged state

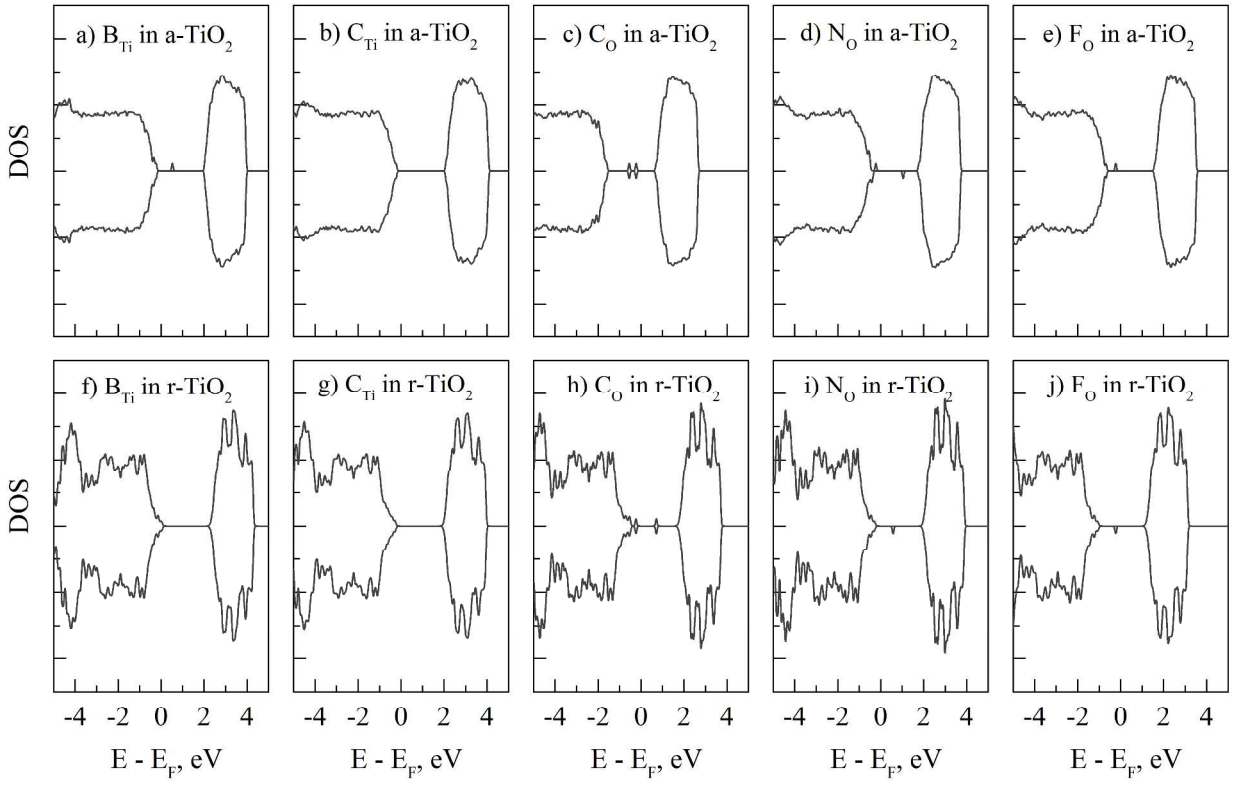

Figure 2. Density of states of amorphous and rutile TiO_2 with substitution of Ti and O by B, C, N and F in their neutral charge states (DFT+U calculations)

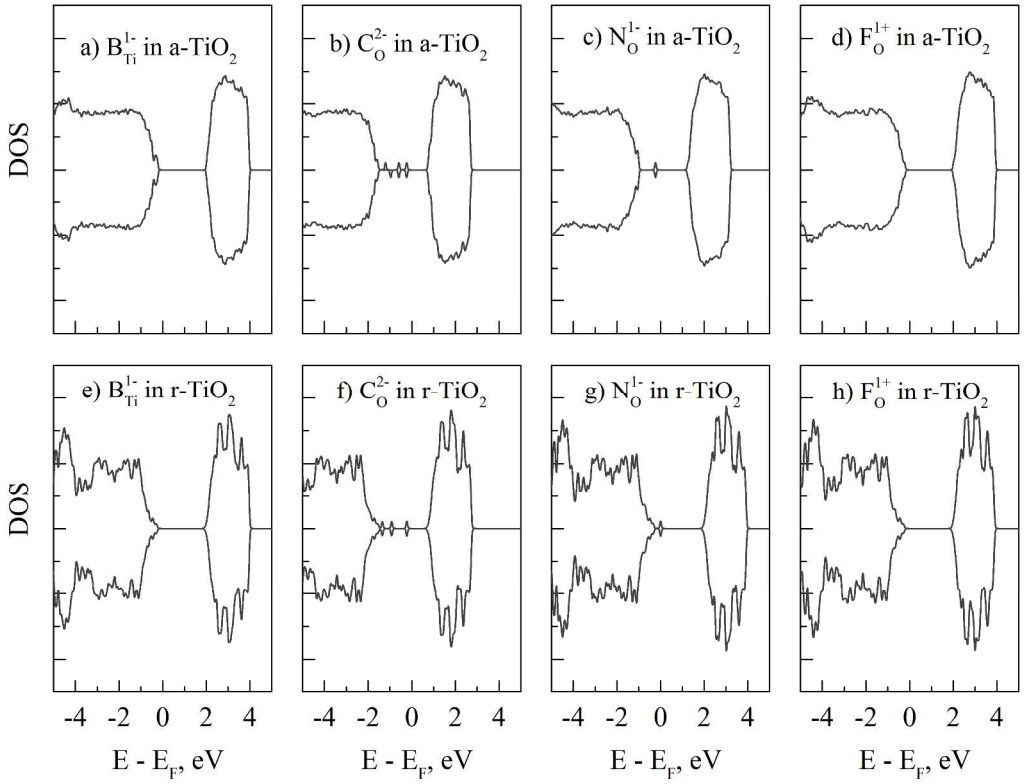

Figure 3. Density of states of amorphous and rutile TiO_2 with substitution of Ti and O by B, C, N and F in their ionic charge states (B_{Ti}^{1-}, C_O^{2-}, N_O^{1-}, F_O^{1+}). The results are plotted from DFT+U calculations

3.2. Examination of charge mobility via the defect channels

We have shown that the amorphous TiO_2 could be more prone to the defect formations than its crystal counterpart r-TiO_2. Many of them have impurity states in the middle of the band gap. It would be interesting to investigate the possibility of using these states as the channels for charge transport. In order to evaluate the charge conductivity, we use the Marcus theory to study the charge hopping rate from one defect site to a neighboring defect site. The concentration of defect substitution is one impurity atom per one supercell (1.5 at. % for B_{Ti} and 0.7 at. % for C_O, N_O, F_O, respectively). The transfer rate therefore corresponds to the hopping from one defect location to its periodic image in the simulation. The charge transfer rate 1/τ, according to the Marcus theory, could be calculated as follows [50]:

$$\tau^{-1} = V_c^2 \sqrt{\frac{\pi}{\lambda k_B T \hbar^2}} \exp\left[-\frac{(\lambda + E_f - E_i)^2}{4\lambda k_B T}\right] \quad (2)$$

where k_B is the Boltzmann constant, $\hbar$ is the Planck constant, T is temperature, λ is the reorganization energy of the system when the charge is conducted from one site to another, and V_c is the electronic coupling between two states involved in the transfer. In our work, this state-state coupling V_c was estimated from the impurity state k-point dispersion in a periodic box. According to a simple one band tight-binding model, the band energy difference between the supercell Γ and X points is $4V_c$. The reorganization energy λ due to the charge transfer is calculated as: $E_N(R_N) + E_{N-1}(R_{N-1}) - E_N(R_{N-1}) - E_{N-1}(R_N)$, where E_N and E_{N-1} are energies for systems with N and N-1 electrons. R_N and R_{N-1} indicate the relaxed atomic structures with respective number of electrons (N and N-1). Since TiO_2 usually can only be doped as n-type, we will study the charge transfer in the n-type cases. Under the n-type situation (Fermi energy close to CBM), the charge states of these defects are B_{Ti}^{1-}, C_O^{2-}, N_O^{1-} and F_O^0. As seen in Figure 3a, B_{Ti}^{1-} results in a clear band gap, thus no inside-band-gap conduction channel would be of interest. Meanwhile, other defects (C_O^{2-}, N_O^{1-} and F_O^0) result in occupied mid-gap states that could possibly be used for hole conduction. In this work, therefore, we will calculate the conductivity that corresponds to the hopping of holes via these otherwise occupied channels.

The E_i and E_f represent the total energy of the system before and after the charge transfer between neighboring defect sites (in this work, we use $E_f = E_i$). Using a random walk formula in a square lattice, the carrier mobility μ can be given from the hopping rate $1/\tau$ as [51]:

$$\mu = 6eb^2/(\tau k_B T) \quad (3)$$

here e is the elementary charge and b is the supercell lattice (which corresponds to the hopping distance in our calculations).

The calculated values of τ and μ for hole transfer via the occupied defect states in amorphous TiO_2 at room temperature are tabulated in Table 1. The DFT+U calculations suggest that the hole transport in this context has relatively slow rate; as a consequence, the conduction of charge carriers is insignificant. In addition to the DFT+U, we also performed additional calculations using the DFT* and HSE06* methods, where the asterisk sign (*) in Table 1 indicates that we used the pre-optimized structures from DFT+U for further computations with DFT and HSE06. By employing this technique, we try to work around the fact that it would be computationally expensive to obtain the relaxed atomic structures for several-hundred-atom systems with hybrid calculations. More specifically, the reorganization energy λ* is calculated

using the formula $E_N(R_N^*) + E_{N-1}(R_{N-1}^*) - E_N(R_{N-1}^*) - E_{N-1}(R_N^*)$. Here R^* represent the fully relaxed structures taken from DFT+U calculations, and the energies E are evaluated using self-consistent HSE06 (or DFT) methods (see Supplemental Information). The coupling constants V_c in the (*) methods are obtained from the band energy difference between the Γ and X points ($4V_c$) from self-consistent HSE06 (or DFT) calculations (performed with the pre-optimized DFT+U configurations). The justification and the accuracy of this procedure were discussed in more details in Ref. [11].

The hybrid calculations (HSE06), in addition, also suggest low conductivity of charge via the defect channels provided by all C_O^{2-}, N_O^{1-} and F_O^0. In general, the observed low mobility could be partially due to the localization nature of these states (Figure 4). Table 1 shows that the hopping rate obtained by DFT is always higher than those from HSE06 and DFT+U methods. This overestimation of electronic conductivity by DFT could be explained by the fact that DFT unarguably fails to describe the occupancy of localized states of d orbitals, which in turn results in a higher electronic coupling between neighboring defect states and a significantly lower hopping barrier (reorganization energy) in the calculation. From this perspective, the DFT+U and HSE expectedly produce a better description of the atomic-like defect charge states. The charge transport predicted by DFT+U and HSE06 are relatively at the same order for $C_O^{2-}$and N_O^{1-}, yet the DFT+U calculations yeilds higher rate and mobility for the F_O^0 case (Table 1). Unfortunately, there are no experimental reports for a head-to-head comparision of these defect-state conductivity data in a-TiO_2, especially for low temperatures. However, given that the hole mobility via bulk conduction in r-TiO_2 is theoretically estimated at about 5.1×10^{-3} ($cm^2\ V^{-1}s^{-1}$) [51], our calculations (by either DFT+U and HSE06) would suggest limited contributions of these defect states to the electronic conductivity in a-TiO_2 in the overall framework. These calculations, on one hand, challenge the hypothesis that the hole conduction in the "leaky" a-TiO_2 [6] could be a result of C or N defects. On the other hand, it would further support the suggestion in our earlier work [11] that oxygen vacancy plays its role here for the "mysterious" hole transfer at an energy level far above the valence band maximum.

Table 1. Hole hopping rate and mobility via defect states (C_O^{2-}, N_O^{1-} and F_O^0) in amorphous TiO_2 (room temperature). The DFT* and HSE06* calculations were performed using the pre-optimized structures from DFT+U

	λ, eV			V_c, meV			Transfer rate τ^{-1} (s^{-1})			Hole mobility μ ($cm^2 V^{-1}s^{-1}$)		
	DFT+U	DFT*	HSE06*	DFT+U	DFT*	HSE06*	DFT+U	DFT*	HSE06*	DFT+U	DFT*	HSE06*
C_O^{2-}	0.90	0.21	1.09	0.63	0.50	0.62	1.1×10^{6}	1.2×10^{9}	1.6×10^{5}	4.9×10^{-6}	5.3×10^{-3}	7.3×10^{-7}
N_O^{1-}	1.07	0.95	1.30	0.28	0.33	0.25	3.8×10^{4}	1.7×10^{5}	3.1×10^{3}	1.7×10^{-7}	7.9×10^{-7}	1.4×10^{-8}
F_O^0	0.67	0.35	1.18	0.35	0.55	0.15	3.8×10^{6}	2.9×10^{8}	3.5×10^{3}	1.7×10^{-5}	1.3×10^{-3}	1.6×10^{-8}

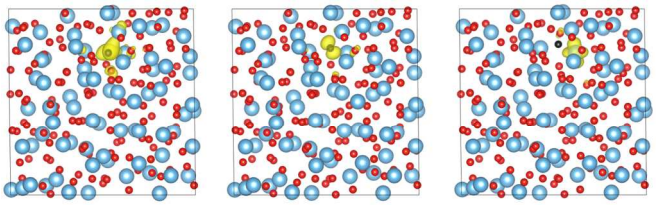

Figure 4. Band decomposed wave function isosurfaces of the defect states (covering 90% of charge) induced by impurities in amorphous TiO_2: a) C_O^{2-} as in Figure 3b, b) N_O^{1-} as in Figure 3c), c) F_O^0 as in Figure 2e. Blue sphere – Ti, red – O, black – corresponding impurity element (C, N or F). The DFT+U calculations are presented

4. Conclusion

In summary, we have investigated the energetics and conductivity of defects states in amorphous titanium dioxide induced by second-row non-metal elements B, C, N and F. The cost of doping in a-TiO_2 could be energetically more favorable (by several eV lower) compared to r-TiO_2, probably as a result of the structural disorder and bonding frustration. Under the n-type situation (Fermi energy close to the conduction band minimum), the substitutions of Ti (by B and C) and O (by C, N and F) possess the charge states as B_{Ti}^{1-}, C_{Ti}^{0}, C_O^{2-}, N_O^{1-} and F_O^0, respectively. Among these defects, only C_O^{2-}, N_O^{1-} and F_O^0 would induce the mid-gap states. Our *ab initio* calculations using the Marcus theory, however, indicate that the hole conduction via these defect channels would be relatively limited. The analysis of charge binding further shows that these

states are quite locally bound, which may partially be responsible for the low conductivity by the hopping mechanism.

Notes

The authors declare no competing financial interests.

ACKNOWLEDGMENTS

This material is based on the work performed by the Joint Center for Artificial Photosynthesis, a DOE Energy Innovation Hub, supported through the Office of Science of the U.S. Department of Energy under Award number DE-SC0004993. We use the resource of National Energy Research Scientific Computing center (NERSC) located in Lawrence Berkeley National Laboratory.

REFERENCES

1. A. Fujishima and K. Honda, *Nature*, 1972, 238, 37-38.
2. X. Chen and S. S. Mao, *Chem Rev*, 2007, 107, 2891-2959.
3. S. K. Deb, *Solid State Commun*, 1972, 11, 713-715.
4. Y. Katsuta, A. E. Hill, A. M. Phahle and Calderwo.Jh, *Thin Solid Films*, 1973, 18, 53-62.
5. Z. Y. Zhang and P. A. Maggard, *J Photoch Photobio A*, 2007, 186, 8-13.
6. S. Hu, M. R. Shaner, J. A. Beardslee, M. Lichterman, B. S. Brunschwig and N. S. Lewis, *Science*, 2014, 344, 1005-1009.
7. S. D. Standridge, G. C. Schatz and J. T. Hupp, *Langmuir*, 2009, 25, 2596-2600.
8. M. Kanna and S. Wongnawa, *Mater Chem Phys*, 2008, 110, 166-175.
9. S. Buddee, S. Wongnawa, U. Sirimahachai and W. Puetpaibool, *Mater Chem Phys*, 2011, 126, 167-177.
10. S. Abedi, B. Karimi, F. Kazemi, M. Bostina and H. Vali, *Org Biomol Chem*, 2013, 11, 416-419.
11. H. H. Pham and L. W. Wang, *Phys Chem Chem Phys*, 2015, 17, 541-550.
12. V. A. Bakaev and W. A. Steele, *Langmuir*, 1992, 8, 1379-1384.
13. V. Petkov, G. Holzhuter, U. Troge, T. Gerber and B. Himmel, *J Non-Cryst Solids*, 1998, 231, 17-30.
14. H. Z. Zhang, B. Chen, J. F. Banfield and G. A. Waychunas, *Phys Rev B*, 2008, 78, 214106.
15. B. Prasai, B. Cai, M. K. Underwood, J. P. Lewis and D. A. Drabold, *J Mater Sci*, 2012, 47, 7515-7521.
16. R. D. Eithiraj and K. R. Geethalakshmi, *Chem Phys Lett*, 2013, 585, 138-142.
17. T. Kohler, M. Turowski, H. Ehlers, M. Landmann, D. Ristau and T. Frauenheim, *J Phys D Appl Phys*, 2013, 46, 325302.
18. M. Landmann, T. Kohler, S. Koppen, E. Rauls, T. Frauenheim and W. G. Schmidt, *Phys Rev B*, 2012, 86, 064201.
19. K. K. Ghuman and C. V. Singh, *J Phys-Condens Mat*, 2013, 25, 475501.
20. L. Liu and X. B. Chen, *Chem Rev*, 2014, 114, 9890-9918.
21. B. Ohtani, Y. Ogawa and S. Nishimoto, *J Phys Chem B*, 1997, 101, 3746-3752.
22. J. P. Rino and N. Studart, *Phys Rev B*, 1999, 59, 6643-6649.
23. H. H. Pham and T. Cagin, *Acta Mater*, 2010, 58, 5142-5149.
24. A. Kellou, H. I. Feraoun, T. Grosdidier, C. Coddet and H. Aourag, *Acta Mater*, 2004, 52, 3263-3271.
25. B. J. Morgan and G. W. Watson, *Phys Rev B*, 2010, 82.
26. J. Wang, D. N. Tafen, J. P. Lewis, Z. L. Hong, A. Manivannan, M. J. Zhi, M. Li and N. Q. Wu, *J Am Chem Soc*, 2009, 131, 12290-12297.
27. C. Di Valentin, G. Pacchioni and A. Selloni, *Phys Rev B*, 2004, 70, 085116.
28. M. Landmann, E. Rauls and W. G. Schmidt, *J Phys-Condens Mat*, 2012, 24.
29. K. A. McDonnell, N. J. English, M. Rahman and D. P. Dowling, *Phys Rev B*, 2012, 86.
30. V. Celik and E. Mete, *Phys Rev B*, 2012, 86.
31. B. H. Q. Dang, M. Rahman, D. MacElroy and D. P. Dowling, *Surf Coat Tech*, 2012, 206, 4113-4118.
32. X. B. Chen, L. Liu, P. Y. Yu and S. S. Mao, *Science*, 2011, 331, 746-750.
33. H. Irie, Y. Watanabe and K. Hashimoto, *J Phys Chem B*, 2003, 107, 5483-5486.

34. D. Morris, Y. Dou, J. Rebane, C. E. J. Mitchell, R. G. Egdell, D. S. L. Law, A. Vittadini and M. Casarin, *Phys Rev B*, 2000, 61, 13445-13457.
35. C. Di Valentin and G. Pacchioni, *Catal Today*, 2013, 206, 12-18.
36. X. X. Yang, C. D. Cao, L. Erickson, K. Hohn, R. Maghirang and K. Klabunde, *Appl Catal B-Environ*, 2009, 91, 657-662.
37. C. L. Muhich, J. Y. Westcott, T. Fuerst, A. W. Weimer and C. B. Musgrave, *J Phys Chem C*, 2014, 118, 27415-27427.
38. M. Matsui and M. Akaogi, *Mol Simulat*, 1991, 6, 239-244.
39. V. V. Hoang, *Phys Status Solidi B*, 2007, 244, 1280-1287.
40. W. Kohn and L. J. Sham, *Phys Rev*, 1965, 140, 1133-1138.
41. G. Kresse and J. Furthmuller, *Phys Rev B*, 1996, 54, 11169-11186.
42. P. E. Blochl, *Phys Rev B*, 1994, 50, 17953-17979.
43. J. P. Perdew, K. Burke and M. Ernzerhof, *Phys Rev Lett*, 1996, 77, 3865-3868.
44. S. L. Dudarev, G. A. Botton, S. Y. Savrasov, C. J. Humphreys and A. P. Sutton, *Phys Rev B*, 1998, 57, 1505-1509.
45. P. M. Kowalski, M. F. Camellone, N. N. Nair, B. Meyer and D. Marx, *Phys Rev Lett*, 2010, 105.
46. H. J. Monkhorst and J. D. Pack, *Phys Rev B*, 1976, 13, 5188-5192.
47. J. Paier, M. Marsman, K. Hummer, G. Kresse, I. C. Gerber and J. G. Angyan, *J Chem Phys*, 2006, 125, 249901.
48. S. Lany and A. Zunger, *Phys Rev B*, 2009, 80, 085202.
49. D. Zherebetskyy and L.-W. Wang, *Advanced Materials Interfaces*, 2014, DOI: 10.1002/admi.201300131, 1300131.
50. R. A. Marcus, *Rev Mod Phys*, 1993, 65, 599-610.
51. N. A. Deskins and M. Dupuis, *J Phys Chem C*, 2009, 113, 346-358.